ARTICLES
https://doi.org/10.1038/s41929-018-0125-2
nature catalysis

Lifetime improvement in methanol-to-olefins catalysis over chabazite materials by high-pressure H_2 co-feeds

Sukaran S. Arora[1], Davy L. S. Nieskens[2], Andrzej Malek[3] and Aditya Bhan[1]*

Mitigating catalyst deactivation in the industrially deployed process of methanol-to-olefins conversion over HSAPO-34 is a critical challenge. Here, we demonstrate that lifetime in methanol-to-olefins catalysis over HSAPO-34 at sub-complete methanol conversion, as determined by the cumulative turnover capacity per Brønsted acid site towards hydrocarbon products in the effluent before complete catalyst deactivation (~15% carbon final conversion), can be enhanced with increasing efficacy (~2.8× to >70×) by co-feeding H_2 at increasing partial pressures (400–3,000 kPa) in the influent with methanol compared with co-feeding helium at equivalent pressures. The lifetime improvement in the presence of high-pressure H_2 co-feeds is observed to be more prominent at complete methanol conversion than at sub-complete conversion. The improvements in catalyst lifetime by co-feeding H_2 are rendered without any deleterious effects on C_2–C_4 olefins selectivity, which remains ~85% carbon irrespective of the inlet H_2 pressure. These observations can be rationalized based on the participation of H_2 in hydrogen transfer reactions, and in effect, the interception of pathways that promote the formation of deactivation-inducing polycyclic species.

Methanol-to-olefins (MTO) catalysis over the proton-form chabazite (CHA)-type zeotype material, HSAPO-34, is commercially deployed as a non-oil-based alternative for the production of light olefins, ethylene and propylene[1–4]. The CHA topology (with large ellipsoidal cages, 10 Å × 6.7 Å, interconnected via narrow eight-membered ring apertures, 3.8 Å × 3.8 Å)[5] of this silico-aluminophosphate material only allows effusion of small-chain linear molecules[6–10] enabling high C_2–C_4 olefins selectivity (>85% carbon) during MTO conversion[11,12]; however, this characteristic also renders this material susceptible to deactivation by the accumulation of unreactive polycyclic aromatic compounds inside the large cages with reaction progress[13–15]. The mechanistic origins of light olefins in auto-catalytic MTO chemistry are described by the hydrocarbon pool mechanism involving olefins and aromatics as organic co-catalytic centres that act as scaffolds for C–C bond formation and scission[6,7,10,13,16]. Formaldehyde production in methanol transfer dehydrogenation events and the resulting alkylation of olefin and aromatic chain carriers by formaldehyde have been implicated in recent reports to play a critical role in the initiation and termination sequences in MTO[17–21]. We surmise that H_2 acts as a hydrogen transfer reagent at high pressures on zeolites/zeotypes (also reported by Meusinger and Corma[22]), and thereby mitigates the transformation of active olefin and monocyclic aromatic organic co-catalysts in MTO to polycyclic species responsible for catalyst deactivation[13,23,24].

We report that co-feeding H_2 at high partial pressures (400–3,000 kPa) with CH_3OH (13 kPa) results in orders of magnitude (~2.8× to >70×) improvement in the catalyst lifetime relative to helium co-feeds at identical pressures under sub-complete conversion conditions. These improvements are afforded while maintaining the high C_2–C_4 olefins selectivity (~85% carbon) attribute of HSAPO-34, irrespective of the H_2 partial pressure in the feed with methanol. Furthermore, varying the inlet concentration of H_2 enables selectivity control over the light olefins distribution in MTO wherein the ethylene-to-propylene molar ratio (E/P) in the effluent is noted to systematically decrease with increasing H_2 partial pressure. Co-feeding H_2 at complete methanol conversion conditions (lower space velocities) exhibits an even more pronounced effect on the cumulative turnover capacity of HSAPO-34 for MTO than at sub-complete conversion conditions. Co-processing H_2 (400 kPa and 1,600 kPa) with CH_3OH over HSSZ-13 (the aluminosilicate analogue of HSAPO-34) and HZSM-5 (an aluminosilicate zeolite with MFI topology) also results in improved catalyst lifetimes (~4.5× and ~3×, respectively), demonstrating that the beneficial effects of co-processing H_2 during MTO are prevalent regardless of the zeolite or zeotype material employed. The observed improvements in catalyst lifetime by co-feeding H_2 can be rationalized by the direct involvement of H_2 in hydrogen transfer reactions in MTO, with increasing efficacy as the inlet partial pressure of H_2 increases. Specifically, we demonstrate in experiments that involve co-processing H_2 with methanol/formaldehyde mixtures that a role of H_2 is to intercept formaldehyde-mediated deactivation pathways, which consequently manifests in longer catalyst lifetimes for MTO conversion.

Results

Effects of H_2 on lifetime and selectivity in MTO catalysis. Co-feeding H_2 at increasing inlet partial pressures (400–3,000 kPa) with CH_3OH (13 kPa) at sub-complete methanol conversion results in a monotonic increase (~2.8× to >70×) in the cumulative turnover capacity (up to a final conversion level of ~15% carbon) of HSAPO-34 for MTO catalysis (see Fig. 1a). The catalyst exhibits far superior performance at the highest partial pressure (3,000 kPa) of H_2 co-feed employed in the study compared with lower influent H_2 concentrations, and is only partially deactivated even after 130 h on stream. The lifetime enhancement factors calculated based on the cumulative turnovers achieved at final conversion levels of ~50 and ~15% carbon with varying H_2 pressures are tabulated in Supplementary Table 1. In contrast with the effects observed with high-pressure H_2 co-feeds, co-feeding high-pressure helium at

[1]Department of Chemical Engineering and Materials Science, University of Minnesota, Minneapolis, MN, USA. [2]Dow Benelux B.V., Hoek, Netherlands. [3]The Dow Chemical Company, Midland, MI, USA. *e-mail: abhan@umn.edu

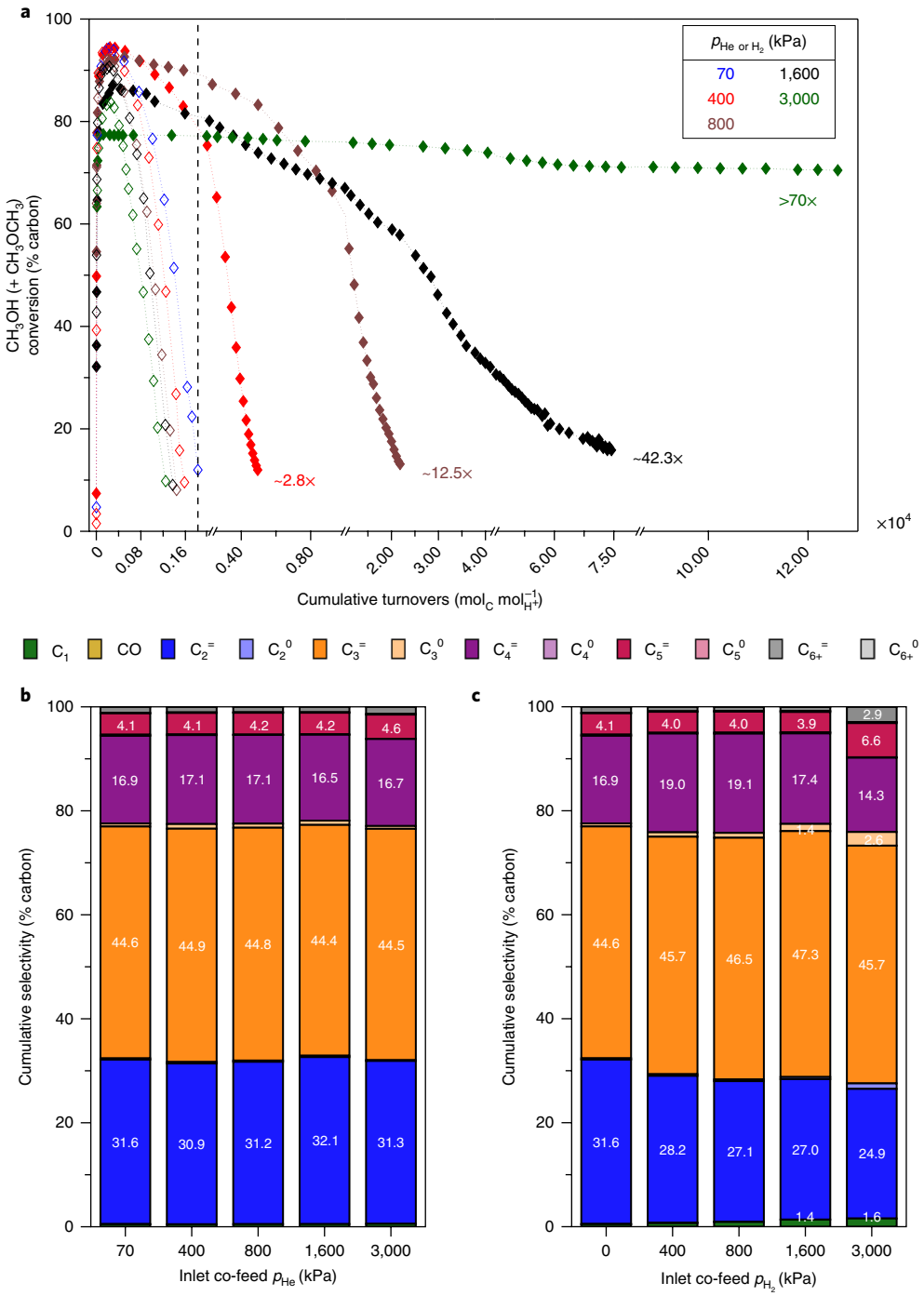

Fig. 1 | Catalytic behaviour of HSAPO-34 with helium versus H_2 co-feeds at sub-complete methanol conversion. a, Methanol (CH_3OH), including DME (CH_3OCH_3), conversion profiles versus cumulative turnovers observed with varying helium (open symbols) or H_2 (filled symbols) co-feeds. The vertical dashed line denotes the cumulative turnover capacity of HSAPO-34 for methanol conversion with helium co-feed at 70 kPa, which is used to calculate the relative lifetime improvement factors with different H_2 co-feeds. **b**,**c**, Cumulative selectivity versus inlet partial pressures of helium (**b**) and H_2 (**c**) co-feeds. Reaction conditions: 4 mg HSAPO-34, 673 K, 13 kPa CH_3OH, 70 kPa helium (≡0 kPa H_2)–3,000 kPa helium; 400–3,000 kPa H_2, 22 kPa argon, 40 $g_{CH_3OH}\ g_{cat}^{-1}\ h^{-1}$. The superscripts '=' and '0' represent olefinic and paraffinic fractions of the respective carbon group.

equivalent pressures is observed to have no influence on the lifetime of HSAPO-34 for methanol conversion (see Fig. 1a), demonstrating unambiguously that the presence of H_2 is paramount for improved catalyst lifetimes in MTO. We note that any effects on the maximum conversion levels (see Fig. 1a) owing to potential catalyst bypass at the high diluent feed rates (1–8 $cm^3\ s^{-1}$) relative to methanol (0.033 $cm^3\ s^{-1}$) required to achieve the desired partial pressures of the respective reagents trend in the same direction irrespective of the diluent identity, helium or H_2 (see Supplementary Fig. 1); the observed decrease in maximum conversion levels with increasing H_2 pressures is therefore unrelated to catalyst lifetime.

Figure 1b,c presents the effects of varying the inlet partial pressures of helium versus H_2 co-feeds, respectively, on the cumulative selectivity of different hydrocarbon products observed in the effluent stream during MTO over HSAPO-34. Cumulative selectivity represents the fractional amount of methanol/DME-derived carbon

Table 1 | E/P and O/P molar ratios with helium versus H_2 co-feeds in MTO

Co-feed	He					H_2				
Partial pressure (kPa)	70	400	800	1,600	3,000	0	400	800	1,600	3,000
E/P	1.06	1.03	1.05	1.08	1.06	1.06	0.93	0.87	0.86	0.82
O/P	40.5	36.2	38.3	37.1	41.0	40.5	29.4	23.5	16.1	10.8

Reaction conditions: 4 mg HSAPO-34, 673 K, 13 kPa CH_3OH, 70 kPa helium (≡0 kPa H_2)–3,000 kPa helium; 400–3,000 kPa H_2, 22 kPa argon, 40 g_{CH_3OH} g_{cat}^{-1} h^{-1}.

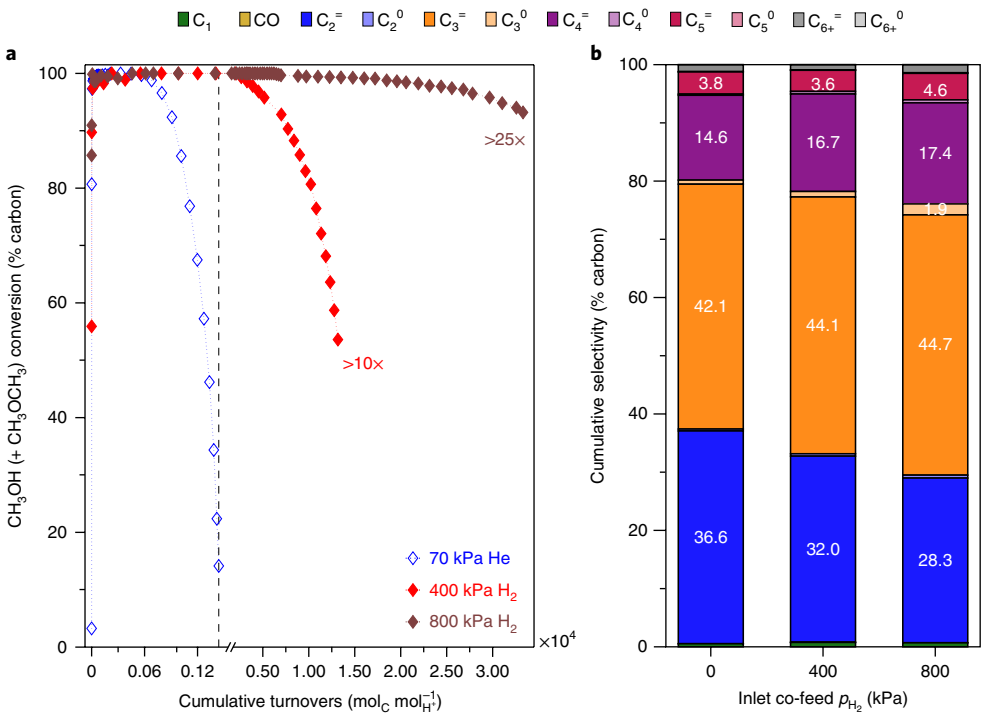

Fig. 2 | Catalytic behaviour of HSAPO-34 with helium versus H_2 co-feeds at complete methanol conversion. a, Methanol (CH_3OH), including DME (CH_3OCH_3), conversion profiles versus cumulative turnovers observed with varying helium or H_2 co-feeds. The vertical dashed line denotes the cumulative turnover capacity of HSAPO-34 for methanol conversion with helium co-feed at 70 kPa, which is used to calculate the relative lifetime improvement factors with different H_2 co-feeds. **b**, Cumulative selectivity versus inlet partial pressures of H_2 co-feeds. Reaction conditions: 27 mg HSAPO-34, 673 K, 13 kPa CH_3OH, 0 kPa H_2 (≡70 kPa helium)–800 kPa H_2, 22 kPa argon, 6 g_{CH_3OH} g_{cat}^{-1} h^{-1}. The superscripts '=' and '0' represent olefinic and paraffinic fractions of the respective carbon group.

atoms observed in a particular product to the total amount observed in all effluent products (C_1–C_{6+}) over the catalyst lifetime. With the exception of the study involving the 3,000 kPa H_2 co-feed, C_2 selectivity is observed to monotonically decrease (31.9–27.4% carbon) while the combined selectivity of C_3 and C_4 is observed to monotonically increase (62.3–66.3% carbon) with increasing influent H_2 partial pressure (0–1,600 kPa). C_{5+} selectivity is observed to exhibit no discernible trend and remains invariant (~5% carbon) with H_2 partial pressure. The lower combined selectivity to C_3–C_4 fractions and higher C_{5+} selectivity in the study with 3,000 kPa H_2 co-feed relative to lower partial pressures of H_2 can be rationalized as a consequence of the lower extent of olefin interconversion reactions at the high conversion levels noted over the entire span of the reaction. Furthermore, cumulative CH_4 selectivity is observed to monotonically increase (0.49–1.57% carbon) with increasing p_{H_2} (0–3,000 kPa); however, the cumulative C_1 selectivity (including CH_4 and CO) is <1.6% carbon at all H_2 partial pressures, which is insignificant compared with the selectivity of C_2–C_4 fractions (~85% carbon). The observed monotonic trends in selectivity with varying H_2 co-feeds are in contrast with the case of helium co-feeds at equivalent conditions where no such perceptible trends are noted.

Table 1 presents the effects of varying H_2 partial pressure on the ethylene-to-propylene molar ratio (E/P) and olefins-to-paraffins molar ratio (O/P) in the effluent hydrocarbon product stream. E/P represents the ratio of the total molar amount of ethylene to the total molar amount of propylene, whereas O/P represents the ratio of the total molar amount of C_2–C_{6+} olefins to the total molar amount of C_1–C_{6+} paraffins, including CH_4, observed over the catalyst lifetime. The monotonic decrease in E/P (1.06–0.82) with increasing H_2 partial pressure (0–3,000 kPa) suggests suppressed rates of propagation of the aromatics-based cycle over its olefins-based counterpart as ethylene is predominantly formed in aromatics-based methylation and dealkylation events during MTO over HSAPO-34 (refs [25,26]). O/P also monotonically decreases (40.5–10.8) with increasing H_2 partial pressure (0–3,000 kPa) but exceeds 10 even at the highest co-fed pressure of H_2, evidencing that the effluent product stream, dominated by C_2–C_4 fractions, is mostly composed of olefins and that co-processing H_2 does not disrupt the high light olefins selectivity characteristic of HSAPO-34 in MTO. In comparison, co-feeding helium at equivalent pressures has no effect on both E/P and O/P.

The relative improvement in the cumulative turnover capacity of HSAPO-34 for MTO with increasing H_2 partial pressure is more

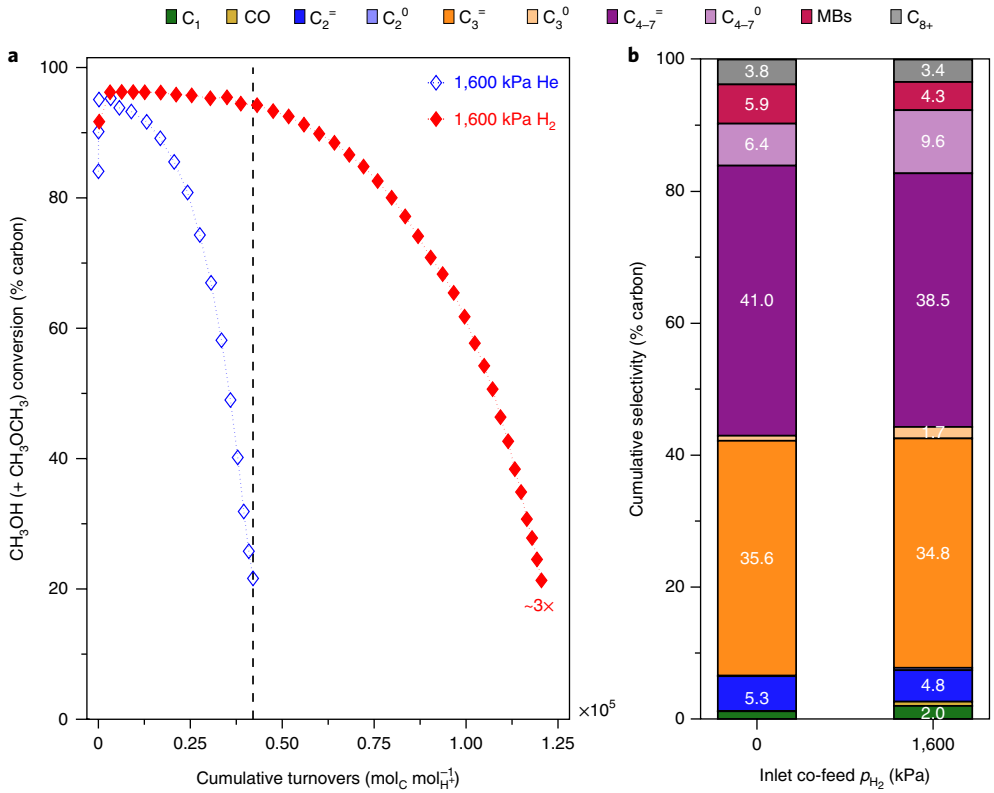

Fig. 3 | Catalytic behaviour of HZSM-5 with helium versus H_2 co-feeds at sub-complete methanol conversion. a, Methanol (CH_3OH), including DME (CH_3OCH_3), conversion profiles versus cumulative turnovers observed with helium or H_2 co-feeds. The vertical dashed line denotes the cumulative turnover capacity of HZSM-5 for methanol conversion with helium co-feed at 1,600 kPa, which is used to calculate the relative lifetime improvement factor with H_2 co-feed at 1,600 kPa. **b**, Cumulative selectivity versus inlet partial pressures of H_2 co-feeds. Reaction conditions: 5 mg HZSM-5, 723 K, 13 kPa CH_3OH, 0 kPa H_2 (≡1,600 kPa helium)–1,600 kPa H_2, 22 kPa argon, 32.1 g_{CH_3OH} g_{cat}^{-1} h^{-1}. The superscripts '=' and '0' represent olefinic and paraffinic fractions of the particular carbon group; 'MBs' represents methyl-substituted benzenes.

significant and more pronounced (>10× versus ~2.8× with 400 kPa H_2 co-feed, and >25× versus ~12.5× with 800 kPa H_2 co-feed; Figs. 1a and 2a) at complete methanol conversion conditions or, equivalently, at lower methanol space velocities (6 g_{CH_3OH} g_{cat}^{-1} h^{-1} versus 40 g_{CH_3OH} g_{cat}^{-1} h^{-1}). This is probably an effect of a lower averaged methanol concentration along the catalyst bed at lower space velocities, which results in lower overall rates of transfer dehydrogenation of methanol and consequently manifests in a lower concentration of formaldehyde—implicated to induce catalyst deactivation[17,19,27,28]. Moreover, analogous to the sub-complete conversion results, C_2–C_4 olefins remain dominant while C_2 selectivity is observed to monotonically decrease (36.9–28.8% carbon) and the combined selectivity of C_3 and C_4 fractions is observed to monotonically increase (57.5–64.5% carbon) with increasing influent H_2 partial pressure (0–800 kPa) (see Fig. 2b).

Effects of H_2 on MTO performance of zeolites other than HSAPO-34. HSSZ-13, the aluminosilicate analogue of HSAPO-34, also exhibits an enhanced MTO lifetime (~4.5×) in the presence of high-pressure H_2 co-feeds (400 kPa) while maintaining high overall light olefins selectivity (>85% carbon) at sub-complete conversion conditions (see Supplementary Fig. 2), evidencing that co-feeding H_2 results in longer catalyst lifetimes for MTO conversion irrespective of the identity of the CHA material employed. HZSM-5, an aluminosilicate material with MFI framework type, also exhibits a significant increase in lifetime (~3×) for methanol conversion in the presence of high-pressure H_2 co-feeds (1,600 kPa) while retaining high olefinic content (78.1% carbon) in the predominant product groups, C_2–C_7 (see Fig. 3). The detailed physical and chemical characteristics of the HZSM-5 sample used in this study have been reported elsewhere[21]. These demonstrations clearly validate the applicability of the proposed strategy of co-feeding high-pressure H_2 to enhance catalyst lifetime during methanol conversion over zeolite materials diverse in composition and topology.

Mechanistic basis for H_2 co-feed effects in MTO. We surmise that the observed improvements in the total turnover capacity of zeolites/zeotypes for MTO conversion by co-processing H_2 probably result from the participation of H_2 in hydrogen transfer reactions with increasing efficacy as the partial pressure of H_2 in the feed increases. Zeolites/zeotypes are lesser-known hydrogenation catalysts relative to metal-based formulations; however, both the ability of H_2 to facilitate hydrogen transfer at high pressures[29–31] and the reversibility of monomolecular alkane dehydrogenation at atmospheric pressure on proton-form zeolites[32] have been documented in the literature. We evidenced the ability of H_2 to participate in hydrogen transfer events in independent studies involving reactions of propylene-H_2 mixtures over HSAPO-34 at MTO-relevant conditions. Co-processing H_2 (400–1,600 kPa) with propylene (2.2 kPa) results in a monotonic increase in both the cumulative turnover capacity of HSAPO-34 for propylene conversion and the cumulative propane selectivity (see Supplementary Fig. 3), consistent with the observed increase in catalyst lifetime and decrease in O/P during MTO catalysis. Furthermore, the catalyst lifetime in MTO has been shown to correlate with the average methanol partial pressure in recent reports demonstrating a higher catalyst lifetime when using: (1) DME versus methanol as feedstock over different zeolite or zeotype catalysts[18,28,33]; (2) continuous stirred tank reactors versus packed-bed reactor configurations

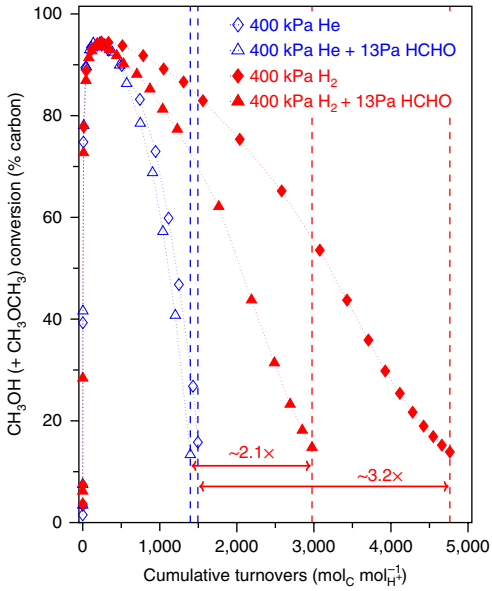

Fig. 4 | Catalytic behaviour of HSAPO-34 with helium versus H_2 co-feeds with methanol-formaldehyde feeds. Reaction conditions: 4 mg HSAPO-34, 673 K, 13 kPa CH_3OH (+13 Pa HCHO (+110 Pa H_2O)), 400 kPa helium, 400 kPa H_2, 40 g_{CH_3OH} g_{cat}^{-1} h^{-1}. The vertical dashed lines denote the cumulative turnover capacity of HSAPO-34 for methanol conversion with and without formaldehyde co-feed when co-processing helium (blue-colored) or H_2 (red-colored).

for methanol conversion over HZSM-5 (ref. [34]); and (3) low inlet methanol partial pressures or high contact times for methanol conversion over HSAPO-34 (ref. [19]). Methanol partial pressure plays a critical role in controlling the extent of transfer dehydrogenation events involving methanol that result in the production of formaldehyde in reference to methylation events involved in carbon chain growth during MTO[19,21]. Formaldehyde is purportedly involved in Prins condensation reactions with olefins and aromatics, resulting in the transformation of active organic co-catalytic species to inactive polycyclic aromatic species[17–19,28]. We demonstrate that co-processing H_2 (400 kPa) with a mixed feed of CH_3OH (13 kPa) and HCHO (13 Pa) over HSAPO-34 also results in an improved catalyst lifetime relative to the case of co-processing helium at equivalent pressures (see Fig. 4). This observation suggests that a probable role of H_2 in MTO, among possible others, is to intercept formaldehyde-mediated alkylation reactions that catalyse the formation of polycyclic aromatic compounds responsible for loss of catalytic activity. An independent study involving chromatographic analysis of the occluded organic species extracted from spent HSAPO-34 samples at sub-complete methanol conversion suggests that co-feeding high-pressure H_2 does not significantly alter the composition of carbon-containing species retained in the catalyst at complete deactivation (see Supplementary Fig. 4). The composition of the extracts in all studies, irrespective of p_{H_2}, is typical of MTO conversion without any H_2 co-feeds over HSAPO-34 reported in the literature wherein pyrenes are observed to be the dominant species in the spent catalysts[24,25].

Relative to existing strategies for improving the MTO lifetime, including the introduction of water co-feeds[35,36], changing process parameters such as the feed methanol pressure and contact-time[19,27], and material parameters such as crystallite size[37,38], acid site density[24,39], introduction of mesoporous domains[40], incorporation of rare earth metal oxides or pure metals and/or their cations[41–43], co-processing H_2 is effective in enhancing the cumulative turnover capacity while sustaining high light olefins selectivity, typical of CHA-type zeolite/zeotype formulations. Our observations in this report also explain the observed stable time-on-stream behaviour of physical mixtures of metal oxide catalysts and HSAPO-34 for high-pressure reactions of CO/H_2 or CO_2/H_2 mixtures for light olefins/paraffins production[44–48].

Conclusions

We demonstrate that co-processing H_2 at high-pressures with CH_3OH over CHA-type zeolite/zeotype catalyst formulations results in marked improvements in the catalyst lifetime (>70×) while preserving the high light olefins selectivity characteristic of these materials during MTO conversion. In independent studies, co-feeding high-pressure H_2 is shown to result in: (1) enhanced formation of propane from propylene feeds over HSAPO-34; and (2) enhanced MTO lifetime of HSAPO-34 in the case of co-reacting CH_3OH and HCHO, thereby suggesting that H_2 participates in hydrogen transfer reactions and, in effect, intercepts alkylation chemistries mediated by HCHO that otherwise result in the transformation of active co-catalytic hydrocarbon pool species to polycyclic aromatic compounds that engender catalyst deactivation during MTO catalysis.

Methods

Catalyst preparation. The templated form of SAPO-34 was formulated by stirring together 8.2 g of aluminium isopropoxide ($Al(OC_3H_7)_3$) with a solution of 3.9 g of 85 wt% orthophosphoric acid in 8.4 g of deionized water. Subsequently, 1.2 g of an aqueous solution of 30 wt% SiO_2 (Ludox AS-30) and 0.5 g of deionized water were stirred into the mixture until a homogeneous consistency was achieved. Finally, 16.8 g of an aqueous solution of 35 wt% tetraethylammonium hydroxide was added to form the reaction mixture. Once formulated, the reaction mixture was placed in a stainless steel stirred Parr reactor and heated to 473 K at 0.0083 K s^{-1}. The temperature was maintained for 120 h under autogenous pressure while stirring at 60 r.p.m. The product was recovered by centrifugation, washed with deionized water and dried at 363 K overnight.

Catalyst characterization. The framework type of the synthesized material was confirmed as CHA by powder X-ray diffraction (see Supplementary Fig. 5).

The overall atomic ratio ((Al + P)/Si = 9.7) was determined from the bulk composition obtained using X-ray fluorescence (see Supplementary Table 2). Measurements obtained from inductively coupled plasma atomic emission spectroscopy and neutron activation analysis indicated the absence of any major metallic impurities in the sample (see Supplementary Table 2).

The atomic ratio in the near-surface region ((Al + P)/Si = 8.1) was determined by X-ray photoelectron spectroscopy and suggests that silicon is homogeneously distributed in the lattice (see Supplementary Fig. 6 for the spectra and Supplementary Table 3 for the atomic composition).

The cubic morphology and average crystallite size (~1 µm) were characterized by scanning electron microscopy (see Supplementary Fig. 7).

The Brunauer–Emmett–Teller surface area (~554 m^2 g^{-1}), and t-plot micropore volume (~0.28 cm^3 g^{-1}) were determined from N_2 adsorption–desorption at 77 K (see Supplementary Fig. 8 and Supplementary Table 4).

^{27}Al, ^{29}Si and ^{31}P magic-angle spinning nuclear magnetic resonance spectra (see Supplementary Table 5 for the experimental conditions and Supplementary Fig. 9 for the spectra) evidenced that: (1) a majority of aluminium and phosphorus atoms were tetrahedrally coordinated in framework positions and located at sites of identical chemical environment; and (2) a majority of silicon atoms were incorporated as isolated sites with tetrahedral coordination to aluminium atoms in framework positions.

The Brønsted acid site density (~1.1 mmol g^{-1}) was enumerated from NH_3 temperature-programmed desorption (see Supplementary Fig. 10 and Supplementary Table 6). Further characterization details are provided in the Supplementary Methods.

Catalytic testing. All experiments were performed in a borosilicate glass-lined stainless steel reactor tube (6.35 mm outer diameter and 4 mm inner diameter; Scientific Glass Engineering). The tubular reactor was placed inside a resistively heated furnace (Model 3210; Applied Test Systems) and the reaction temperature was measured using a K-type thermocouple (KMTXL-020U; Omega) wrapped around the reactor periphery with the tip placed near the axial-centre and regulated with an electronic controller (Watlow 96). The as-synthesized uncalcined SAPO-34 sieve fractions (180–420 µm), diluted with quartz sand sieve fractions (150–420 µm; subject to a previous wash in 2 M HNO_3, a deionized water rinse and treatment in flowing dry air at 1,273 K for 12 h; ≤0.15 g_{cat} g_{sand}^{-1}; Acros Organics), were packed into the middle heated zone of the reactor between quartz wool plugs before the reactor was placed in the furnace. To avoid displacement of the catalyst under high-pressure gas flows, the remaining reactor volume was filled with quartz rods (3 mm outer diameter). Before every experiment, the starting catalyst material was converted to its proton form by in situ thermal treatment in flowing dry air (1.67 cm^3 s^{-1}; Minneapolis Oxygen) at 823 K (0.0167 K s^{-1} ramp rate) for 6 h before being allowed to cool down to 673 K

and being subject to a helium (1.67 $cm^3 s^{-1}$; Minneapolis Oxygen, 99.997%) purge at 673 K for ≥2 h. The total gas-phase pressure (measured using a pressure transducer (0–6,890 kPag; Omega PX32B1-1KGV) placed upstream of the reactor and connected to a digital reader (Omega DP25B-E)) was controlled using a back-pressure regulator (0–3,440 kPag; Tescom 44–2300 series) placed downstream of the reactor. All gas flows, including H_2 (Matheson, 99.999%), helium (Minneapolis Oxygen, 99.997%), C_3H_6 (5% in balance helium; Praxair, Certified Standard) and argon (Matheson, 99.9993%), were metered using mass flow controllers (Brooks 5850E). Depending on the operating conditions, liquid reagents, including CH_3OH (Fluka, ≥99.9%), HCHO (16% w/v in H_2O; Pierce), deionized water or mixtures thereof, were delivered either using a stainless steel syringe (Harvard Apparatus) or a glass syringe (Scientific Glass Engineering), driven by a PHD ULTRA XF syringe pump (Harvard Apparatus) or a Legato 100 syringe pump (KD Scientific), respectively. The liquids were fed and evaporated in heat-traced lines (353 K) and swept by the flowing gas stream. Reactor effluent stream compositions were quantified using a gas chromatograph (Agilent GC 7890A) equipped with a dimethylpolysiloxane HP-1 column (50 m × 320 μm × 0.52 μm) connected in parallel to a flame ionization detector and a mass spectrometer (Agilent MSD 5975C) for detecting hydrocarbons and oxygenates, and a GS-GasPro column (60 m × 320 μm) connected to a thermal conductivity detector for detecting permanent gases (H_2, argon and CO). The partial pressure of methanol in the feed was kept fixed at 13 kPa by feeding methanol at a constant flow rate of 0.033 $cm^3 s^{-1}$ (gas phase) while varying the inlet flow rate of the diluent (helium or H_2) from 1 to 8 $cm^3 s^{-1}$ and the total gas-phase pressure of the combined feed from 435–3,035 kPa to achieve the desired partial pressures of the diluent (400–3,000 kPa). Argon was used as the internal standard and its flow rate was kept fixed at 0.056 $cm^3 s^{-1}$, corresponding to a partial pressure of 22 kPa under the employed operating conditions. Methanol conversion was calculated based on the total carbon content observed in the effluent hydrocarbon products excluding dimethyl ether (DME).

Data availability. The data that support the plots within this paper and other findings of this study are available from the corresponding author upon reasonable request.

Received: 27 February 2018; Accepted: 10 July 2018;
Published online: 24 August 2018

References

1. Chen, J. Q., Bozzano, A., Glover, B., Fuglerud, T. & Kvisle, S. Recent advancements in ethylene and propylene production using the UOP/Hydro MTO process. *Catal. Today* **106**, 103–107 (2005).
2. Mokrani, T. & Scurrell, M. Gas conversion to liquid fuels and chemicals: the methanol route-catalysis and processes development. *Catal. Rev.* **51**, 1–145 (2009).
3. Yilmaz, B. & Müller, U. Catalytic applications of zeolites in chemical industry. *Top. Catal.* **52**, 888–895 (2009).
4. Tian, P., Wei, Y., Ye, M. & Liu, Z. Methanol to olefins (MTO): from fundamentals to commercialization. *ACS Catal.* **5**, 1922–1938 (2015).
5. Baerlocher, C., McCusker, L. B. & Olson, D. *Atlas of Zeolite Framework Types* (Elsevier, Amsterdam, 2007).
6. Song, W., Haw, J. F., Nicholas, J. B. & Heneghan, C. S. Methylbenzenes are the organic reaction centers for methanol-to-olefin catalysis on HSAPO-34. *J. Am. Chem. Soc.* **122**, 10726–10727 (2000).
7. Song, W., Fu, H. & Haw, J. F. Supramolecular origins of product selectivity for methanol-to-olefin catalysis on HSAPO-34. *J. Am. Chem. Soc.* **123**, 4749–4754 (2001).
8. Arstad, B. & Kolboe, S. Methanol-to-hydrocarbons reaction over SAPO-34. Molecules confined in the catalyst cavities at short time on stream. *Catal. Lett.* **71**, 209–212 (2001).
9. Arstad, B. & Kolboe, S. The reactivity of molecules trapped within the SAPO-34 cavities in the methanol-to-hydrocarbons reaction. *J. Am. Chem. Soc.* **123**, 8137–8138 (2001).
10. Song, W., Marcus, D. M., Fu, H., Ehresmann, J. O. & Haw, J. F. An oft-studied reaction that may never have been: direct catalytic conversion of methanol or dimethyl ether to hydrocarbons on the solid acids HZSM-5 or HSAPO-34. *J. Am. Chem. Soc.* **124**, 3844–3845 (2002).
11. Nawaz, S., Kvisle, S., Lillerud, K.-P., Stocker, M. & Øren, H. Selectivity and deactivation profiles of zeolite type materials in the MTO process. *Stud. Surf. Sci. Catal.* **61**, 421–427 (1991).
12. Yuen, L.-T., Zones, S. I., Harris, T. V., Gallegos, E. J. & Auroux, A. Product selectivity in methanol to hydrocarbon conversion for isostructural compositions of AFI and CHA molecular sieves. *Microporous Mater.* **2**, 105–117 (1994).
13. Haw, J. F., Song, W., Marcus, D. M. & Nicholas, J. B. The mechanism of methanol to hydrocarbon catalysis. *Acc. Chem. Res.* **36**, 317–326 (2003).
14. Schulz, H. "Coking" of zeolites during methanol conversion: basic reactions of the MTO-, MTP- and MTG processes. *Catal. Today* **154**, 183–194 (2010).
15. Olsbye, U. et al. Conversion of methanol to hydrocarbons: how zeolite cavity and pore size controls product selectivity. *Angew. Chemie Int. Ed.* **51**, 5810–5831 (2012).
16. Marcus, D. M. et al. Experimental evidence from H/D exchange studies for the failure of direct C–C coupling mechanisms in the methanol-to-olefin process catalyzed by HSAPO-34. *Angew. Chemie Int. Ed.* **45**, 3133–3136 (2006).
17. Müller, S. et al. Hydrogen transfer pathways during zeolite catalyzed methanol conversion to hydrocarbons. *J. Am. Chem. Soc.* **138**, 15994–16003 (2016).
18. Martinez-Espin, J. S. et al. New insights into catalyst deactivation and product distribution of zeolites in the methanol-to-hydrocarbons (MTH) reaction with methanol and dimethyl ether feeds. *Catal. Sci. Technol.* **6**, 2314–2331 (2017).
19. Hwang, A., Kumar, M., Rimer, J. D. & Bhan, A. Implications of methanol disproportionation on catalyst lifetime for methanol-to-olefins conversion by HSSZ-13. *J. Catal.* **346**, 154–160 (2017).
20. Martinez-Espin, J. S. et al. Hydrogen transfer versus methylation: on the genesis of aromatics formation in the methanol-to-hydrocarbons reaction over H-ZSM-5. *ACS Catal.* **7**, 5773–5780 (2017).
21. Arora, S. S. & Bhan, A. The critical role of methanol pressure in controlling its transfer dehydrogenation and the corresponding effect on propylene-to-ethylene ratio during methanol-to-hydrocarbons catalysis on H-ZSM-5. *J. Catal.* **356**, 300–306 (2017).
22. Meusinger, J. & Corma, A. Activation of hydrogen on zeolites: kinetics and mechanism of *n*-heptane cracking on H-ZSM-5 zeolites under high hydrogen pressure. *J. Catal.* **152**, 189–197 (1995).
23. Guisnet, M. & Magnoux, P. Organic chemistry of coke formation. *Appl. Catal. A* **212**, 83–96 (2001).
24. Marcus, D. M., Song, W., Ng, L. L. & Haw, J. F. Aromatic hydrocarbon formation in HSAPO-18 catalysts: cage topology and acid site density. *Langmuir* **18**, 8386–8391 (2002).
25. Hereijgers, B. P. et al. Product shape selectivity dominates the methanol-to-olefins (MTO) reaction over H-SAPO-34 catalysts. *J. Catal.* **264**, 77–87 (2009).
26. Hwang, A., Prieto-Centurion, D. & Bhan, A. Isotopic tracer studies of methanol-to-olefins conversion over HSAPO-34: the role of the olefins-based catalytic cycle. *J. Catal.* **337**, 52–56 (2016).
27. Keil, F. Methanol-to-hydrocarbons: process technology. *Microporous Mesoporous Mater.* **29**, 49–66 (1999).
28. Martinez-Espin, J. S. et al. Benzene co-reaction with methanol and dimethyl ether over zeolite and zeotype catalysts: evidence of parallel reaction paths to toluene and diphenylmethane. *J. Catal.* **349**, 136–148 (2017).
29. Kanai, J., Martens, J. A. & Jacobs, P. A. On the nature of the active sites for ethylene hydrogenation in metal-free zeolites. *J. Catal.* **133**, 527–543 (1992).
30. Senger, S. & Radom, L. Zeolites as transition-metal-free hydrogenation catalysts: a theoretical mechanistic study. *J. Am. Chem. Soc.* **122**, 2613–2620 (2000).
31. Zheng, A., Liu, S.-B. & Deng, F. Chemoselectivity during propene hydrogenation reaction over H-ZSM-5 zeolite: insights from theoretical calculations. *Microporous Mesoporous Mater.* **121**, 158–165 (2009).
32. Gounder, R. & Iglesia, E. Catalytic hydrogenation of alkenes on acidic zeolites: mechanistic connections to monomolecular alkane dehydrogenation reactions. *J. Catal.* **277**, 36–45 (2011).
33. Li, Y., Zhang, M., Wang, D., Wei, F. & Wang, Y. Differences in the methanol-to-olefins reaction catalyzed by SAPO-34 with dimethyl ether as reactant. *J. Catal.* **311**, 281–287 (2014).
34. Müller, S. et al. Coke formation and deactivation pathways on H-ZSM-5 in the conversion of methanol to olefins. *J. Catal.* **325**, 48–59 (2015).
35. Marchi, A. & Froment, G. Catalytic conversion of methanol to light alkenes on SAPO molecular sieves. *Appl. Catal.* **71**, 139–152 (1991).
36. Wu, X. & Anthony, R. Effect of feed composition on methanol conversion to light olefins over SAPO-34. *Appl. Catal. A* **218**, 241–250 (2001).
37. Nishiyama, N. et al. Size control of SAPO-34 crystals and their catalyst lifetime in the methanol-to-olefin reaction. *Appl. Catal. A* **362**, 193–199 (2009).
38. Chen, D., Moljord, K. & Holmen, A. A methanol to olefins review: diffusion, coke formation and deactivation on SAPO type catalysts. *Microporous Mesoporous Mater.* **164**, 239–250 (2012).
39. Zhu, Q. et al. The study of methanol-to-olefin over proton type aluminosilicate CHA zeolites. *Microporous Mesoporous Mater.* **112**, 153–161 (2008).
40. Schmidt, F., Paasch, S., Brunner, E. & Kaskel, S. Carbon templated SAPO-34 with improved adsorption kinetics and catalytic performance in the MTO-reaction. *Microporous Mesoporous Mater.* **164**, 214–221 (2012).
41. Salmasi, M., Fatemi, S. & Najafabadi, A. T. Improvement of light olefins selectivity and catalyst lifetime in MTO reaction; using Ni and Mg-modified SAPO-34 synthesized by combination of two templates. *J. Ind. Eng. Chem.* **17**, 755–761 (2011).
42. Sedighi, M., Ghasemi, M. & Jahangiri, A. Catalytic performance of CeAPSO-34 molecular sieve with various cerium content for methanol conversion to olefin. *Korean J. Chem. Eng.* **34**, 997–1003 (2017).
43. Hwang, A. & Bhan, A. Bifunctional strategy coupling Y_2O_3-catalyzed alkanal decomposition with methanol-to-olefins catalysis for enhanced lifetime. *ACS Catal.* **7**, 4417–4422 (2017).
44. Jiao, F. et al. Selective conversion of syngas to light olefins. *Science* **351**, 1065–1068 (2016).

45. Cheng, K. et al. Direct and highly selective conversion of synthesis gas into lower olefins: design of a bifunctional catalyst combining methanol synthesis and carbon–carbon coupling. *Angew. Chemie Int. Ed.* **55**, 4725–4728 (2016).
46. Gao, P. et al. Direct conversion of CO_2 into liquid fuels with high selectivity over a bifunctional catalyst. *Nat. Chem.* **9**, 1019–1024 (2017).
47. Li, Z. et al. Highly selective conversion of carbon dioxide to lower olefins. *ACS Catal.* **7**, 8544–8548 (2017).
48. Nieskens, D. L. S., Ciftci, A., Groenendijk, P. E., Wielemaker, M. F. & Malek, A. Production of light hydrocarbons from syngas using a hybrid catalyst. *Ind. Eng. Chem. Res.* **56**, 2722–2732 (2017).

Acknowledgements

We acknowledge: The Dow Chemical Company and National Science Foundation (CBET 1701534) for financial support; the Characterization Facility, University of Minnesota, which receives partial support from the National Science Foundation through the Materials Research Science and Engineering Centers programme, for providing the X-ray diffraction and X-ray photoelectron spectroscopy data; T. Whitmer, The Ohio State University, for providing the NMR data; The Dow Chemical Company, Analytical Science, Midland and Terneuzen for providing the quantitative elemental analysis, scanning electron microscopy and extracts analysis data; D. M. Millar, The Dow Chemical Company, for synthesis of the SSZ-13 sample; and J. F. DeWilde, The Dow Chemical Company, for helpful technical discussions.

Author contributions

D.L.S.N. and A.M conceptualized the research effort. The experimental outline was designed by all authors. A.M. synthesized the SAPO-34 sample. S.S.A. performed the experiments. S.S.A. and A.B. analysed the reaction data. All authors contributed towards data interpretation. S.S.A. drafted the initial manuscript. All authors reviewed and edited the manuscript and supplementary materials.

Competing interests

The authors declare no competing interests.

Additional information

Supplementary information is available for this paper at https://doi.org/10.1038/s41929-018-0125-2.

Reprints and permissions information is available at www.nature.com/reprints.

Correspondence and requests for materials should be addressed to A.B.

Publisher's note: Springer Nature remains neutral with regard to jurisdictional claims in published maps and institutional affiliations.